17th World Conference on Earthquake Engineering, 17WCEE
Sendai, Japan - September 13th to 18th 2020

SEISMIC PERFORMANCE COMPARISONS BETWEEN REINFORCED CONCRETE BUILDINGS AND STEEL BUILDINGS

V. Boonyapinyo [(1)], T. Hinlad [(2)]

[(1)] *Associate Professor, Thammasat University, Pathumthani, Thailand, E-mail: bvirote@engr.tu.ac.th*

[(2)] *Graduate Student, Thammasat University, Pathumthani, Thailand, E-mail: tananut.hin@gmail.com*

Abstract

This research is to investigate the seismic performance comparisons between masonry infilled reinforced concrete buildings and steel buildings located in Chiang Mai, Thailand. To get accurate results, the analytical model was verified with the existing experimental test of the one-span, two-story, flexure-critical reinforced concrete frame. The analytical models are considered for all types of failure modes of buildings, i.e., shear failure, flexural to shear failure, and flexural failure, beam-column joint connection, infill wall and foundation. The masonry infilled walls were modeled by a single-strut model. The seismic performance evaluations are investigated by two methods for comparisons. The first method is by the nonlinear static pushover analysis (NSP) with the capacity spectrum method (CSM). The second method is by the concept of equivalent single degree of freedom (ESDOF) by the incremental dynamic analysis (IDA). The results found that this ESDOF method can reduce the computational time about 93%. The numerical examples are performed on the 5-story apartment reinforced concrete buildings and steel buildings located in Chiang Mai, Thailand. Two types of moment resisting frames were designed, namely, intermediate ductile frames (IDF) with R=5 and gravity load designed (GLD) frames. The results from pushover curve found that the base shear over-strength of IDF concrete building and steel building are 2.10 and 2.70, respectively, compared with the design base shear. The results also found that the steel buildings have more capacity and ductility compared with reinforced concrete buildings. The analysis results of base shear and roof displacement by NSP with CSM agree fairly with the results by IDA of ESDOF.

Keywords: seismic performance, reinforced concrete buildings, steel buildings, masonry infilled wall

1. Introduction

Many researches were studied on non-linear analysis of reinforced concrete framed structures subjected to earthquake excitations. As a consequence, several researchers and designers are interested in nonlinear static (pushover) analysis more than nonlinear dynamic (time history) analysis (NTHA) of multi-degree of freedom structure (MDOF), because the later procedure required a lot of resources and time-consuming. To reduce analysis times of NTHA of the MDOF, Vamvatsikos and Cornell [l] proposed another method that describes a non-linear static (pushover) combined with NTHA of equivalent single degree of freedom (ESDOF). FEMA [2] investigated the effect of stiffness and strength degradation on the seismic response of the structures by using concept of ESDOF. However, all these procedures require accuracy of nonlinear force–deformation curves. In order to capture structural member behavior in non-linear elastic, the model which considers a shear force, a bending moment, and an axial force should be studied. The research related to the model was suggested in the previous works [3-5]. The new standard for the building design under seismic loading in Thailand [6] defines three types of moment frames systems namely ordinary moment frames, intermediate ductile frames and special ductile frames (OMF, IDF and SDF).

This study aimed to evaluate and compare the performance of concrete and steel moment resisting frames. 5 story apartment buildings, namely, intermediate ductile frames (IDF) with R=5 and gravity load designed (GLD) frames and GLD were designed according to [6] and detailing by the provisions of [7] and [8]. A computer-intensive procedure that offers demand and capacity prediction capability by using a series of nonlinear dynamic analyses under 20 suitably multiplied scaled ground motion. Analytical models of buildings are developed using nonlinear finite element program [9].

2. Case Study for 5 story Reinforced Concrete and Steel Buildings

In this study, based on the strong column-weak beam designed concept, plastic hinges (PHs) should be employed on beam elements in order to dissipate the energy generated by earthquakes. The strength ratio between beams and columns in [10] is given as:

$$\sum M_{nc} \geq 1.2 \sum M_{nb} \tag{1}$$

Where $\sum M_{nc}$ is the total nominal flexural strength and also the minimum flexural strength considering the axial and lateral forces of columns connected to a joint; and $\sum M_{nb}$ is the total nominal flexural strength of beams connected to the joint considering the floor reinforcement.

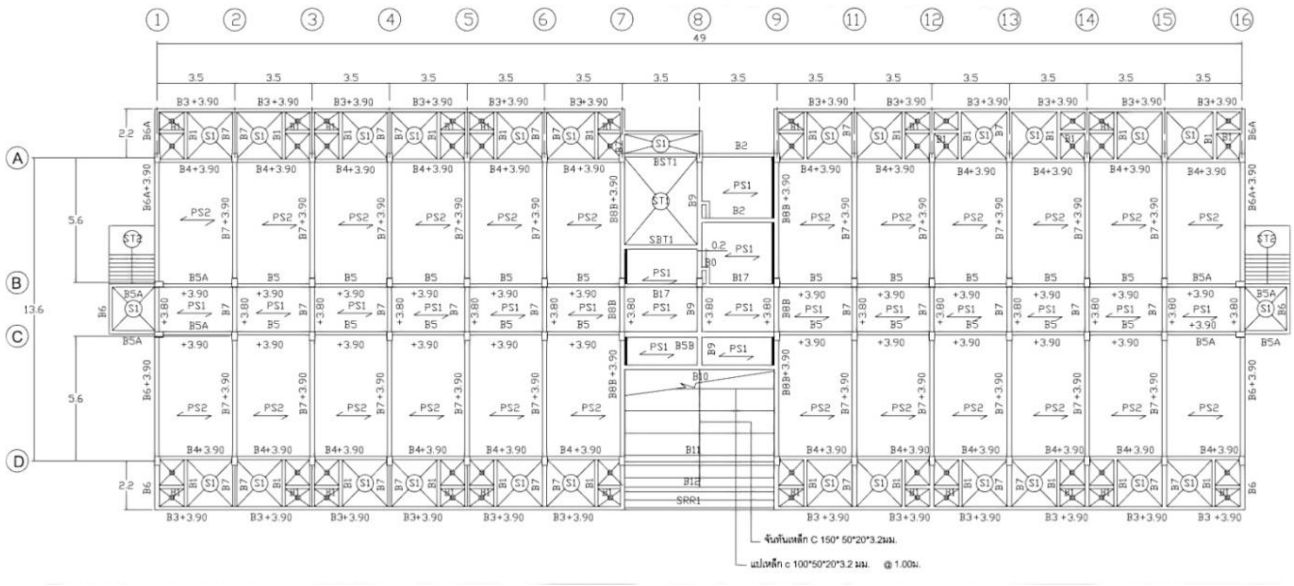

Fig. 1 - Plan view of 5 story building.

Table 1 – Cross-section summaries designed for gravity load design (GLD) building of concrete and steel buildings.

Concrete building					Steel building		
Story	**Type**	**Size (m.)**	**Reinforcement**	**Stirrup**	**Story**	**Type**	**Section Property**
1-2	C1	0.30x0.40	10-db20	Rb6mm.@20cm. Rb6mm.@20cm.	1-2	SC2	W-248x249x8x13 mm.Thk
3-5	C2	0.25x0.40	8-db16	Rb6mm.@20cm. Rb6mm.@20cm.	3-5	SC3	W-200x200x8x12 mm.Thk
1-4	B1	0.25x0.45	6-db16 T 6-db16 B	Rb6mm.@20cm. Rb6mm.@20cm.	GF-1	SB1	W-400x200x8x13 mm.Thk
1-4	B4	0.25x0.45	4-db16 T 4-db16 B	Rb6mm.@20cm. Rb6mm.@20cm.	2-4	SB2	W-300x150x5.5x8 mm.Thk
Roof	B8	0.25x0.45	3-db16 T	Rb6mm.@20cm.	Roof	SB3	W-298x149x5.5x8 mm.Thk

Fig. 1 shows the plan view of 5-story dormitory building used for study. The selected buildings are beam–column reinforced concrete frame without shear wall. The rectangular plan of building measures 13.60x49.00 m. Each story height is 2.80 m. with a total height 14.00 m. The structural system is essentially symmetrical.

Table 2 – Cross-section summaries designed for immediate ductile frame (IDF) building of concrete and steel buildings.

Concrete Building					**Steel Building**		
Story	**Type**	**Size (m.)**	**Reinforcement**	**Stirrup**	**Story**	**Type**	**Section Property**
1-2	C1	0.30x0.50	14-db20	3Rb9mm@15cm. 3Rb9mm@20cm.	1-3	SC2	W-400x400x13x21mm.Thk
3-5	C1	0.30x0.50	14-db20	3Rb9mm@15cm. 3Rb9mm@20cm.	3-5	SC3	W-250x250x9x14 mm.Thk
1-2	B3	0.30x0.60	5-db20 T 5-db20 B	Rb9mm@10cm. Rb9mm@15cm.	GF-1	SB1	W-340x250x9x14 mm.Thk
2-4	B2	0.25x0.50	4-db20 T 4-db20 B	Rb9mm@10cm. Rb9mm@15cm.	2-4	SB2	W-294x200x8x12 mm.Thk
Roof	B1	0.20x0.40	2-db20 T 2-db20 B	Rb9mm@10cm. Rb9mm@15cm	Roof	SB3	W-300x150x6.5x9 mm.Thk

Two types of moment resisting frame were designed, namely gravity load designed (GLD) and intermediate ductile frames (IDF) with R=5, in order to examine the influence of the design ductility classes as moment resisting frames. Each pile is of I-shaped 0.40 m. in size and 21m. in length. It is designed for a vertical safe load of 40 tons, the dimension of beam and column are shown in Tables 1 and 2. In the design, the cylinder compressive strengths of concrete columns and beams are 240 ksc. The yield strengths of steel deformed and rounded bars are 4,000 ksc. (SD 40) and 2,400 ksc. (SR 24), respectively. For seismic evaluation, the actual yield strength of steel reinforcement of 4,600 ksc. (SD 40) and 3,480 ksc. (SR 24) are used for SD 40 and SR 24, respectively [11]. For steel building, the yield strength is 2,500 ksc (SM400).

3. Analytical Model

3.1 Plastic hinge setting of beam and columns

The Plastic hinges (PHs) settings of the beams and columns of the frame were established using the method developed by Sung et al. [3]. For a specific RC component, the relationship between the moment and curvature $(M-\phi)$, can be established when considering the flexural capacity of the component, as shown in Fig. 2 Note that the condition where the shear capacity of the RC component decreases as inelastic deformation proceeds is also included in this approach. As a result, the shear capacity, which consists of the relationship between the transformed moment (M_v) and rotation (θ), as shown in Fig. 2(b), can be obtained. By superimposing the diagrams of $(M_b-\theta)$ and $(M_v-\theta)$, three different types of failure modes (shear failure, flexure to shear failure, and flexure failure) can be illustrated. The PH characteristics indicated by points A through E in Fig. 3, expressed by the relationship between moment and flexural rotation, are therefore definable.

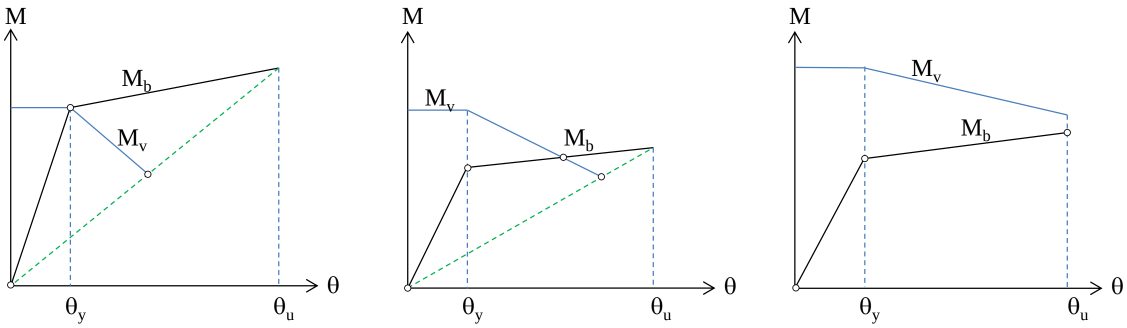

(a) Shear failure (b) Flexure to shear failure (c) Flexure failure

Fig. 2 - Failure modes of a column or beam and their plastic hinge characteristics.

3.2 Plastic hinge settings for beam-column-joints

The plastic hinge (PH) characteristics of beam-column-joints (BCJs) were established using the method developed by Sung et al [4], according to FEMA-356 [12], the nominal shear strength of BCJs can be calculated as

$$V_n = \lambda\gamma\sqrt{f_c^{'}}A_j \quad \text{(psi.)} \tag{2}$$

Where λ is the coefficient of the concrete, and is set as 1 for regular concrete and 0.75 for lightweight concrete; γ is a constant depending on the volumetric ratio of the horizontal confinement reinforcement in the joint and the classification of the BCJ. Specific values of γ can be found in FEMA-356 [12], where $f_c^{'}$ is the ultimate strength of concrete and A_j is the effective cross sectional area of the joint.

Based on FEMA-356 [12], the values used to define the PH characteristics of BCJs are calculated as shown in Fig. 3, where A_j is the initial point and B_j represents the yielding. The initials stiffness of the PH between A_j and B_j equal to 0.4 E_cA_g by assuming that the beam-column joints are part of the column. Since shear failure is a common cause of failure of a BCJs, the strength at point C_j, the final point of the nonlinear stage, is conservatively set as the same value as at B_j. Point D_j is defined to represent the residual strength, and the strength and axial displacement can be estimated as the mean values at points C_j and E_j, where the strength at E_j is 0.2 P_n. The BCJ is simulated by using a pair of cross struts in the diagonal direction when resisting horizontal loading, as illustrated in Fig. 3. The adjacent components of the BCJ are simulated by a rigid bar with a hinge connection on the end point, where the height of the model is the depth of the beam, and the width equals the effective width of the column. The complex behavior of the BCJ is subsequently simulated by a cross-strut model with an equivalent two-force component.

The relationship between the horizontal shear force V and displacement δ is transformed into the direction of the strut, and is derived as

$$P_{strut} = V/2\cos\theta \tag{3}$$

$$\delta_{strut} = \delta\times\cos\theta \tag{4}$$

Where P_{strut} is the equivalent axial force on the strut; V is the equivalent horizontal shear force on the strut; δ_{strut} is the equivalent axial displacement; δ is the equivalent horizontal displacement; and θ is the angle of the strut from horizontal.

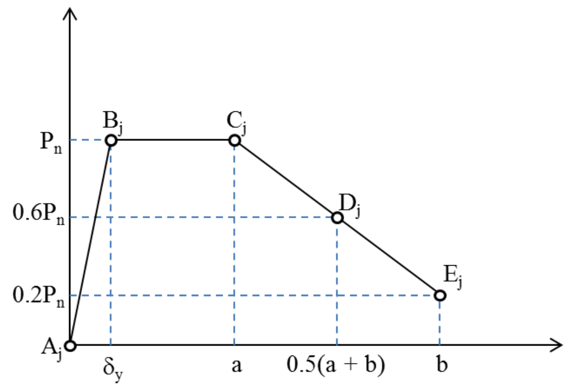

Fig.3 - Behavior of the PH of a beam-column joints.

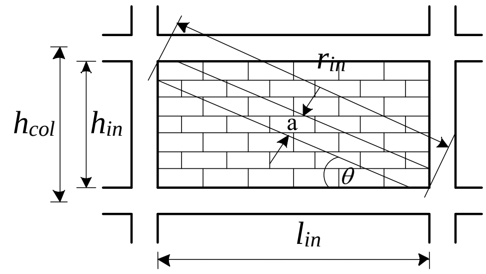

Fig. 4 - Equivalent diagonal compression strut model

3.3 Masonry infill wall

As mentioned earlier, equivalent strut concept will be used to model masonry infill wall. Based on this concept, the stiffness contribution of infill wall is represented by an equivalent diagonal compression strut as shown in Fig. 4. Thickness and modulus of elasticity of strut are assumed to be the same as those of infill wall. Moreover, width of equivalent strut, is determined, which was suggested by FEMA-273 [13].

$$a = 0.175(\lambda_1 h_{col})^{-0.4} r_{in} \tag{5}$$

$$\lambda_1 = [E_{me} t_{in} \sin 2\theta / (4E_{fe} I_{col} h_{in})]^{1/4} \tag{6}$$

Where E_{me} is modulus of elasticity of masonry infill wall, E_{fe} is modulus of elasticity of frame material, I_{col} is moment of inertia of column section, t_{in} is thickness of infill panel.

The axial compression strength of equivalent strut R_s can be obtained by solving equation as shown.

$$R_s = [\tau_0 / (1-\mu_f(h_{in}/l_{in}))] r_{in} t_{in} \tag{7}$$

Where τ_0 is an average value of cohesive strength, r_{in} is length of diagonal of infill panel, t_{in} is thickness of infill panel, μ_f is a typical value for the coefficient of friction, h_{in} is height of infill panel and l_{in} is length of infill panel. In SAP 2000, equivalent diagonal compression strut is modeled as an axial element having a nonlinear axial hinge along its length.

4. Comparisons between Pushover Solutions and Experiments

To verify the analytical models used in this study, the analytical models emphasize on the plastic hinges (PHs) in beams and columns. Three types of PHs were studied include shear failure, flexure to shear failure, and flexure failure, and validation of pushover analysis requires comparison of numerical results with those of the experiments.

The experiments of the one-span, two-story, flexure-critical reinforced concrete frame was tested by Vecchio and Emara [14] to gain further insight into the magnitude and influence of shear deformations in flexure-critical frame structures and to assess the accuracy of analytical procedures developed. The frame was constructed with a centre-to-centre span of 3500 mm, a story height of 2000 mm and an overall height of 4600 mm as shown in Fig. 4. All beams and columns were 300 mm wide and 400 mm deep, while the base was 800 mm wide and 400 mm deep. The frame was built integral with a large, heavily reinforced concrete base to create an essentially fixed foundation. The base was fixed to the lab floor using ten pairs of bolts which were post-tensioned to prevent slip

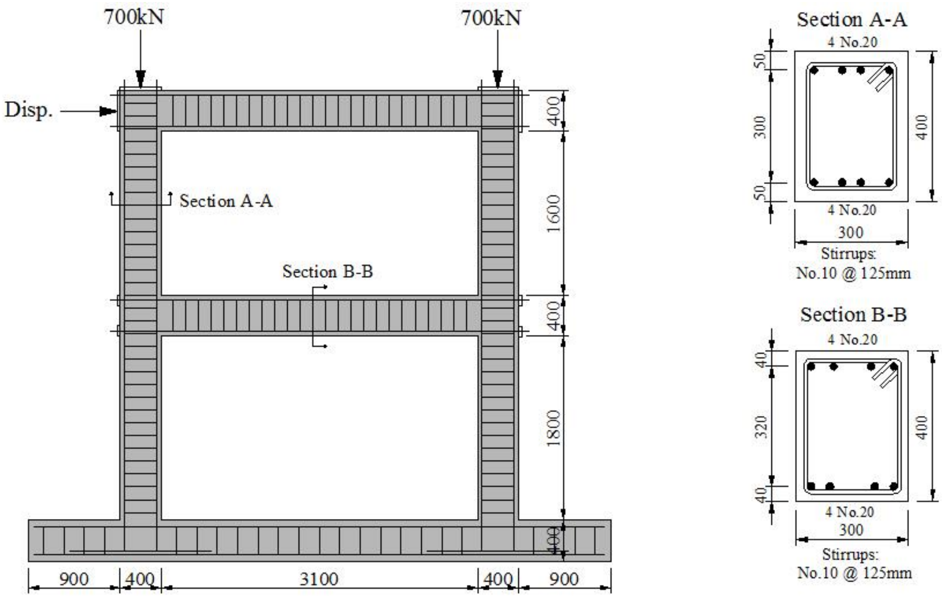

Fig. 5 - Details of Vecchio and Emara Frame for experiments [14].

The testing of the frame involved applying an axial load of 700 kN to each column, maintained constant throughout the test, while monotonically applying a lateral load to the second story beam until the ultimate capacity of the frame was reached. The column loads were provided by two pairs of 450 kN capacity hydraulic jacks, applied through two transverse beams in the force-controlled mode. The lateral load was provided by a 1,000 kN capacity actuator, mounted laterally against a reacting strong wall, in a displacement mode.

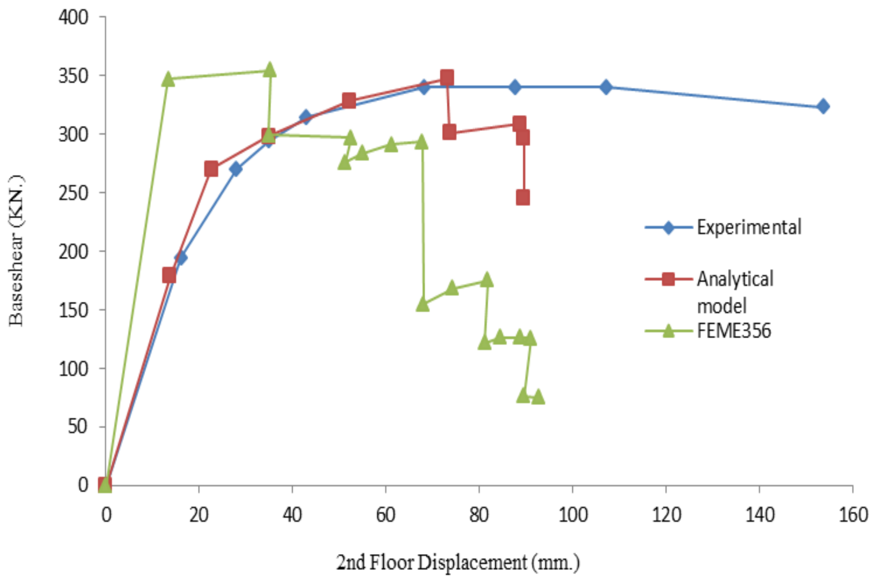

Fig. 6 - Comparisons between pushover curves and experiments for Vecchio and Emara Frame [14].

As shown in Fig. 6, the differences in the initial stiffness, strength, and ductility of the structure were investigated. Default PHs settings in FEMA-356, the green line illustrating the model without considering the BCJ effect expresses the higher stiffness and the ultimate strength is overestimated throughout the whole nonlinear region, which reflects the main drawback of traditional methods that cannot describe the degradation phenomena. Unlike the curve predicted by FEMA-356 which a significant difference occurred throughout the entire process, an accurate result can be obtained by the proposed analytical method, compared with the experimental results.

5. Nonlinear Static Pushover Analysis of Concrete Building and Steel Building

The static pushover analysis is performed on each model to evaluate the lateral strength and post-yield behavior. Displacement-control loading is applied to the models by using a load pattern based on fundamental period of the structures to account the lateral response of the buildings. The pushover curve for one bay frame in Fig. 7 and Table 3 found that the base shear over strength of concrete building and steel building for intermediate ductile frames (IDF) with R=5 are 2.01 and 2.75, respectively. The over strength is ratio of available base shear to required design base shear. The IDF steel building has more capacity and ductility compared with IDF concrete building

Table 3 – Performance of concrete buildings and steel buildings with two types of moment resisting frames, namely, IDF with R=5 and GLD frames by nonlinear static push over analysis

Structure	Design base shear (kg)	Displacement (m)	Base shear (kg)	Over strength
RC,GLD	-	0.139	57,117	-
RC,R5	46,359	0.253	93,003	2.01
ST,GLD	-	0.248	53,765	-
ST,R5	37,842	0.488	104,166	2.75

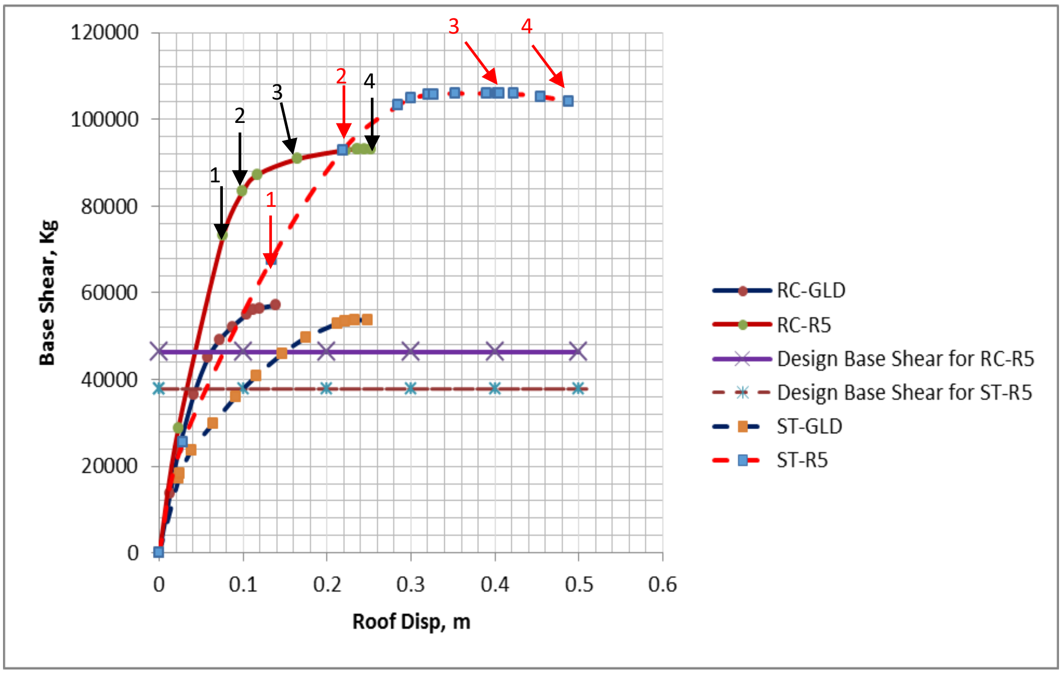

Fig. 7 - Comparisons of base shear capacity and roof displacement between masonry infilled reinforced concrete buildings (RC) and steel buildings (ST) for intermediate ductile frames (IDF) with R=5 and gravity load designed (GLD) frames

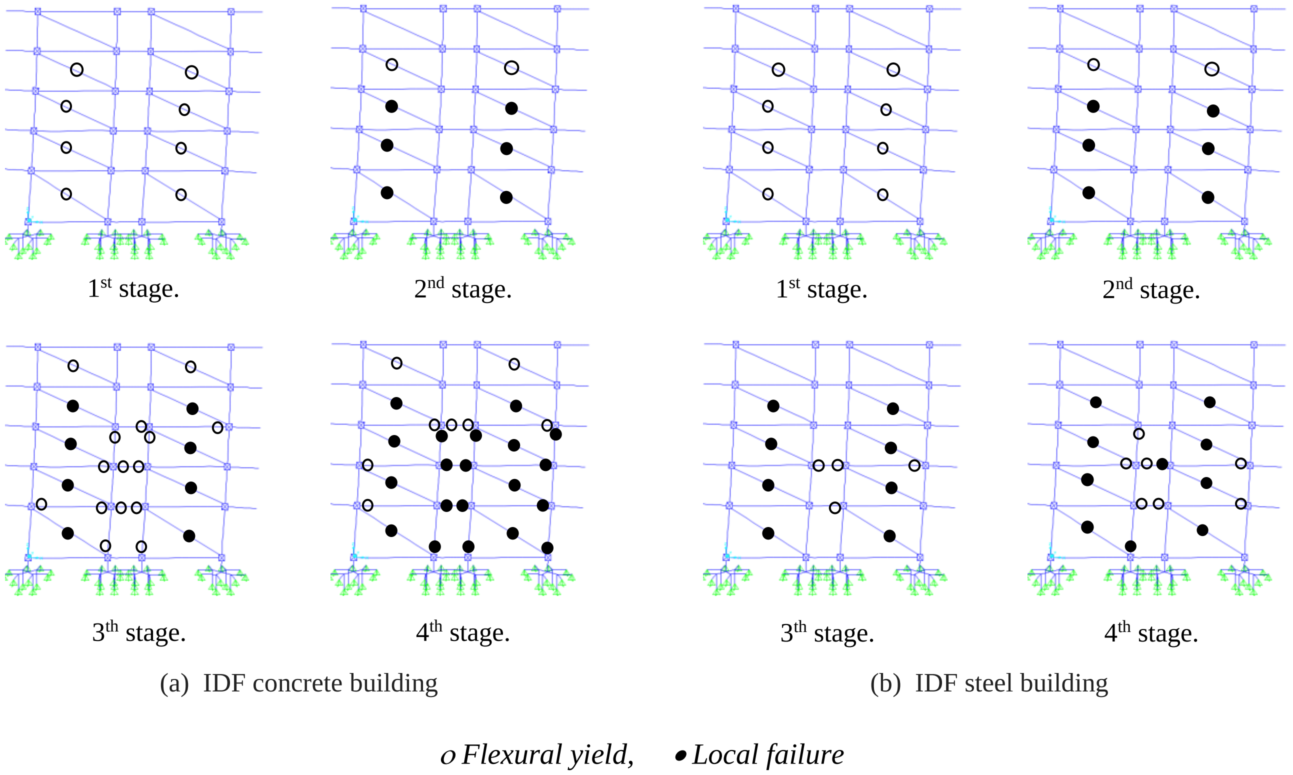

Fig. 8 - Hinge mechanism patterns in IDF concrete and steel buildings (see with Fig. 7).

Fig.8 shows hinge mechanism pattern in IDF steel building. At the beginning, the relationship between base shear and lateral roof displacement represents a linear relationship. Until continue loading of lateral force over elastic period result in the yielding of short beam and the rupture of brick wall. These phenomena led to a few reductions of lateral force resistance. The most reduction of lateral force resistance can be observed when the failures of long beam occurred. All of the failure of long beam appears at the right-side tail because of the vertical force from self-weight load and live load. The vertical forces cause the negative moment at bilateral tails while the lateral force cause the positive moment in long beam at position near the lateral force at the left side.

The lateral force induces the destructive of the moment at the left side. The negative moment at the right side of long beam can be generated, result in the supplement of negative moment at the tail. Since the positive and negative moment resistances long beam were equal, negative moment at right side tail can reach the maximum moment resistance and failure first.

The loss of vertical and lateral resistance force of the structure at failure condition can be occurred when there are great damages in the joint until the stability of the building occurs. Based on the strong column weak beam concept design, there is a little damage in the columns. Displacement coefficient between the layers of the building is a variable that can be described how structure behavior responded and where is the most movement between the layers occurred. The result from nonlinear static pushover analysis also shown that the most inter-story drift can be observed at the second floor. The lateral load capacity of GLD and IDF concrete building were 37.04 %W and 51.20 %W (W = total building weight), respectively.

6. Incremental Dynamic Analysis of Concrete Building

Incremental Dynamic Analysis (IDA) of multi degree of freedom (MDOF) was firstly reported by Vamvatsikos and Cornell [15]. IDA involves performing a series of nonlinear dynamic analyses of a structural model for multiple records by scaling each record to several levels of intensity that are suitably selected to uncover the full range of the model's behavior: from elastic to yielding and nonlinear inelastic, finally leading to global dynamic instability. Each dynamic analysis can be characterized by at least two scalars, an intensity measure (IM), which represents the scaling factor of the record [e.g., the 5% damped first-mode response spectrum acceleration S_a (T_1, 5%)] and an engineering demand parameter (EDP), which monitors the structural response of the model [e.g., peak inter-story drift ratio θ_{max}].

The results from Incremental dynamic analysis of equivalent single degree of freedom are shown in figure 9. It can be interpreted as follow: at the beginning, the linearity was controlled by initial stiffness, so no distributions of the data until the earthquake violence reach up to the yield point. In this stage, some beams are reaching yield point so slope of IDA decrease. Then, the strength of the structure was improved until reach the maximum pushover curve. At this point, IDA slope was going to flat line which was implying that the structure was dynamic instability.

The IDA curves display a wide range distribution of data. Thus, it is essential to summarize randomness of data and quantify introduced by the records. The central value (e.g., the median) was used for easy interpretation of data. Consequently, it has been chosen to calculate the 16%, 50% and 84% fractile values of DM and IM capacity for each limit-state. For example, summarized capacities for each limit-state for 5-storey buildings are shown in Fig. 10.

Dynamic characteristics of these aforementioned buildings could be readily observed through the use of median IDA curves. As it is seen, linear slope is increased as behavior factor is decreased through the models. That is, IDF is the laterally stiffest since its members are designed stronger in comparison with other types of building. Other information may be extracted from IDA curves to pronounce the suitability and capability of moment frames as show in Table 4.

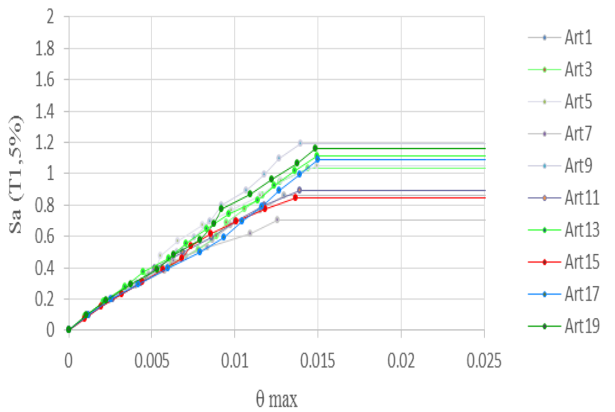

a.) Gravity load design

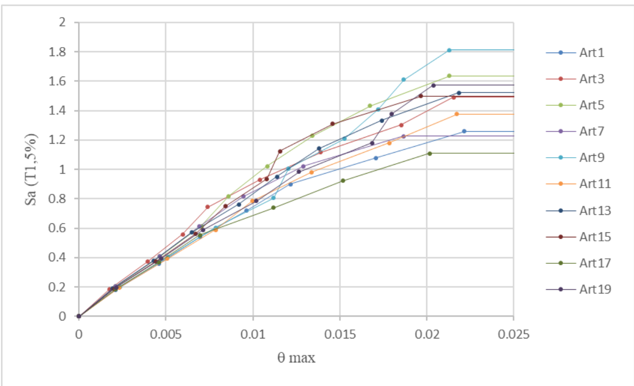

b.) Intermediate ductile frames, R = 5

Fig.9 - All twenty IDA curve for 5-story concrete buildings.

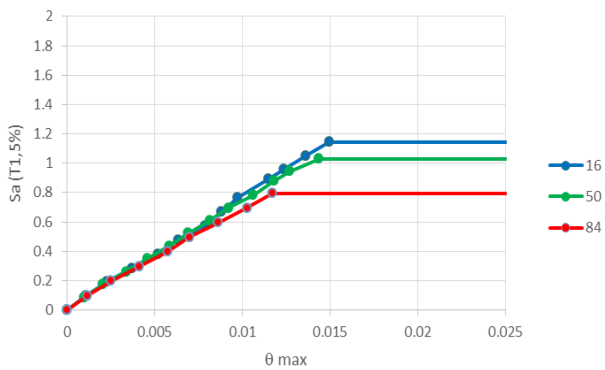

a.) Gravity load design

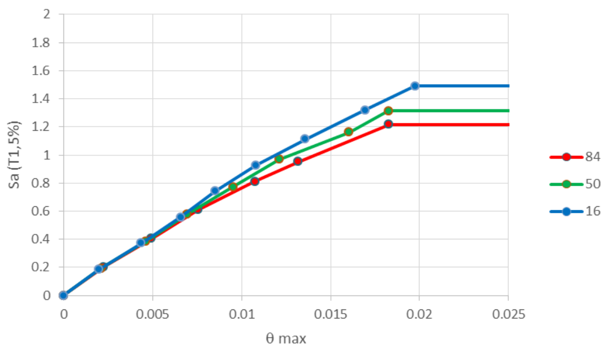

b.) Intermediate ductile frames, R = 5

Fig.10 - The summary of the IDA curves to their 16%, 50% and 84% fractile

Table 4 – Performance of concrete buildings with intermediate ductile frame (IDF) with R=5 and gravity load design (GLD) frame by incremental dynamic analysis

Type	Stage	Period (sec)	Response spectra S_a (T_1, 5%) (g)	Roof displacement (m.)	Base shear (kg.)
GLD	yield	0.844	0.28	0.040	45,621
IDF	yield	0.790	0.52	0.065	57,117
GLD	ultimate	0.844	1.03	0.125	50,536
IDF	ultimate	0.790	1.31	0.151	91,893

Finally, it should be noted that this study applied the concept of equivalent single degree of freedom (ESDOF) for evaluating the seismic performance of the studied building by the mean of incremental dynamic analysis (IDA). The results found that this method can reduce the computational time from 90 minutes per load case for multi degree of freedom (MDOF) to 6 minutes per load case for ESDOF. It reduced about 93% of computational time.

7. Capacity Spectrum Method

The capacity spectrum method (CSM) [16] is used for evaluate performance of structures. The procedure of CSM is as follows. Firstly, by converting the base shears and roof displacements from a non-linear pushover to equivalent spectral accelerations and displacements and then superimposing an earthquake demand curve, the non-linear pushover becomes a capacity spectrum. The earthquake demand curve is represented by response spectra, plotted with different levels of "effective" or "surrogate" viscous damping (e.g. 5%, 10%, 15%, 20% and sometimes 30% to approximate the reduction in structural response due to the increasing levels of damage). Finally, by determining the point, where this capacity spectrum "breaks through" the earthquake demand as show in Fig.11, engineers can develop an estimate of the spectral acceleration, displacement, and damage that may occur for specific structure responding to a given earthquake.

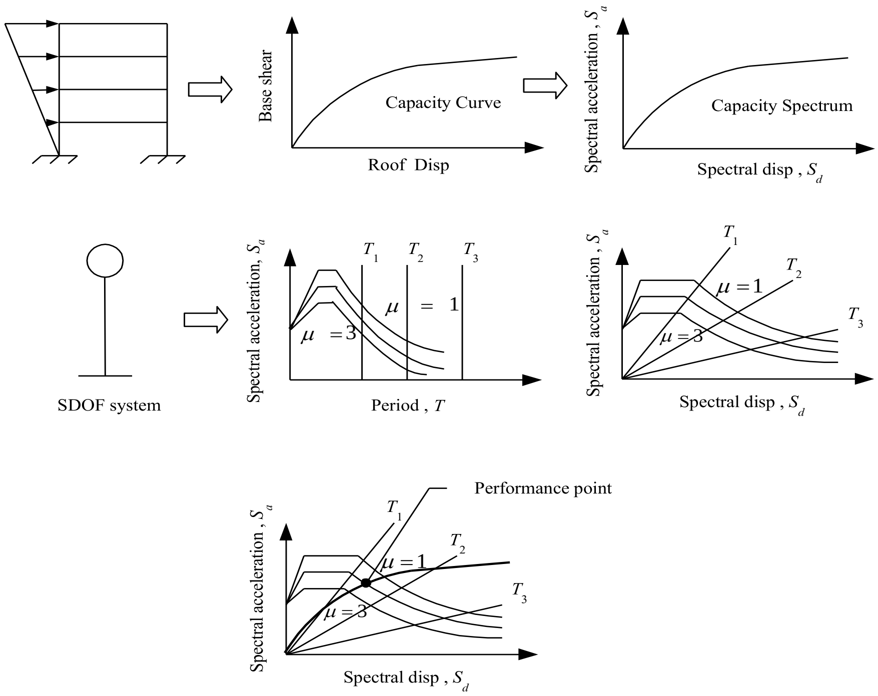

Fig. 11 - The procedure of CSM to estimate of the response of the structure

From the capacity spectrum method (CSM) results, the performance of the frames can be obtained from the intersection of the demand curve and capacity curve as shown in Figs. 12 and 13 and Table 5. The intermediate ductile frames (IDF) has significantly higher reserve strength than gravity load designed (GLD) frames during lateral loading as show in Table 5.

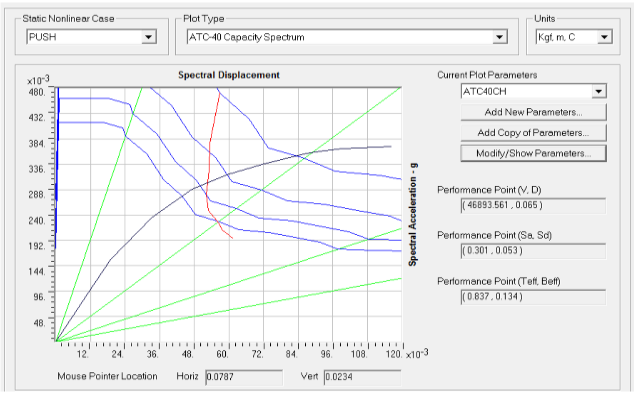

Fig.12: Performance point of GLD concrete building at yield stage by capacity spectrum method

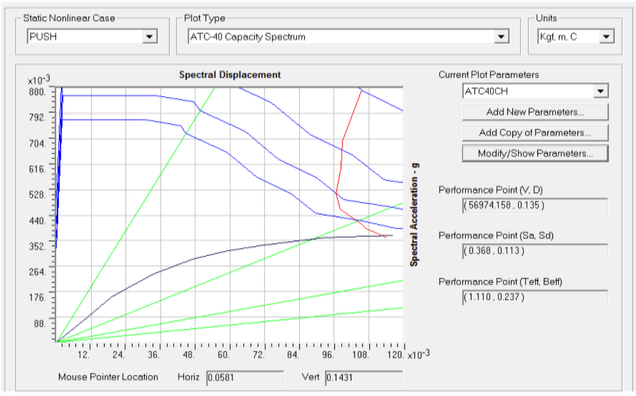

Fig.13: Performance point of GLD concrete building at collapse stage by capacity spectrum method

Table 5 –Performance of concrete building and steel building with intermediate ductile frames (IDF) with R=5 and gravity load designed (GLD) frames by capacity spectrum method (CSM).

Structure	**Stage**	**Roof displacement (m)**	**Base shear (kg)**	**Period at collapse (T_{eff}) (s)**	**Spectral acceleration S_a (g)**
RC,GLD	Yield	0.060	45,621	0.820	0.293
	Ultimate	0.135	56,974	1.110	0.368
RC,R5	Yield	0.066	66,093	0.750	0.375
	Ultimate	0.116	86,862	0.879	0.491
ST,GLD	Yield	0.097	40,742	1.109	0.313
	Ultimate	0.260	53,408	1.474	0.398
ST,R5	Yield	0.104	66,732	0.903	0.510
	Ultimate	0.233	104,050	1.080	0.805

8. Conclusions

This study involves seismic performance and evaluations of 5-story apartment reinforced concrete buildings and steel buildings, two types of moment resisting frames are designed, namely, intermediate ductile frames (IDF) with R=5 and gravity load designed (GLD) frames with infill wall. These buildings were designed according to Thailand seismic code [6]. The analytical models used in this study emphasize on the plastic hinges in beams and columns. Three types of PHs were studied include shear failure, flexure to shear failure, and flexure failure. Based on this study, seismic performance for all buildings can be summarized as follow:

(1) From pushover curve, the base shear over strength of concrete building and steel building for IDF with R=5 are 2.10 and 2.70, respectively, compared with the design base shear.

(2) As far as the effect of the ductility class is concerned concrete building and steel building with IDF ductility classes are to perform satisfactorily during a design earthquake. It demonstrated the successful application of the strong-column–weak-beam implemented in the capacity design for IDF. The IDF steel building has more capacity and ductility compared with IDF concrete building

(3) The lateral load capacity of GLD and IDF of concrete buildings were 37.04 %W and 51.20%W, respectively. The average response spectrum by incremental dynamic analysis (IDA) at the collapse state for GLD and IDF are 1.03 g and 1.31 g, respectively. All of frames are able to resistant a design earthquake.

(4) Using the concept of ESDOF for evaluating the seismic performance of the studied building by the mean of IDA can reduce the computational time from 90 minutes per load case for multi degree of freedom (MDOF) to 6 minutes per load case for ESDOF. It reduced about 93% of computational time.

(5) The analysis results of base shear and roof displacement by the nonlinear static pushover analysis (NSP) with the capacity spectrum method (CSM) agree fairly with the results by the incremental dynamic analysis (IDA) of the equivalent single degree of freedom (ESDOF).

Acknowledgements

This research was partially, financially supported by the Thailand Research Fund (TRF).

References

[1] Vamvatsikos D. and Cornell C. A. (2005): *Seismic performance, capacity and reliability of structures as seen through incremental dynamic analysis*. Department of civil and environmental engineering, Stanford University.

[2] FEMA (2009): Effects of strength and stiffness degradation on seismic response. *Report No. FEMA-P440A*, Federal emergency management agency, Department of homeland security (DHS).

[3] Sung Y.C., Liu KY, Su CK, Tsai IC, and Chang KC.(2005) : A study on pushover analyses of reinforced concrete columns. *Journal of Structural Engineering and Mechanic*, 21(1), p. 35–52.

[4] Sung Y.C., Lin T.K., Hsiao C.C., Lai M.C. (2013) : Pushover analysis of reinforced concrete frames considering shear failure at beam-column joints. *Earthquake Engineering and Engineering Vibration*, Vol.12, No.3, p. 373-383.

[5] Sharma AK., Reddy G.R., Vaze K.K., Eligehausen R. : Pushover experiment and analysis of a full scale non-seismically detailed RC structure. *Engineering Structures*, Vol.46, 2013.

[6] DPT.(2009): Standard for building designed under seismic load. *Report No. DPT 1302-52*, Department of Public works and town and country planning (in Thai).

[7] UBC.(2007): Uniform building code, structural engineering designed provisions. *Report No. UBC 1997*, International Conference of Building Officials (ICBO).

[8] DPT. (2011): Additional standard for building designed under seismic load. *Report No. DPT 1301-54*, Department of Public Works and Town and Country Planning (in Thai).

[9] SAP 2000 (2000): *Integrated finite element analysis and design of structure*: Analysis reference, Computers and Structures, Inc., Berkeley, California.

[10] ACI. (2011): Building code requirements for structural concrete and commentary. *Report No. ACI 318-11*, Farmington Hills, Michigan, U.S.A., American concrete Institute.

[11] Kiattivisanchai S. (2011): *Evaluation of seismic performance of an existing medium-rise reinforced concrete frame building in Bangkok,* M.Eng thesis, Thesis No. ST-01-11, Asian Institute of technology.

[12] FEMA.(2000): Pre-standard and commentary for the seismic rehabilitation of buildings. *Report No. FEMA-356*, Building seismic safety council, Washington D.C.

[13] FEMA.(1997): Guidelines for the seismic rehabilitation of building. *Report No. FEMA-273*, NEHRP Commentary on the guidelines for the seismic rehabilitation of building. *Report No. FEMA-274*, Federal emergency management agency. Washington D.C.

[14] Vecchio F. J.and Emara M. B. (1997): Shear Deformations in Reinforced Concrete Frames, *ACI Structural Journal*, 89-S6,p.46-56

[15] Vamvatsikos D., Cornell C. A. (2002): Incremental dynamic analysis, *Earthquake Engineering and Structural Dynamics*, 31(3), p. 491–514.

[16] Chopra A., & Goel R. (1999): *Capacity-Demand-Diagram Method For Estimate Seismic Deformation of Inelastic Structure: SDF System*. College of Engineering, University of California Berkeley. California.

